J Therm Anal Calorim (2015) 120:1009–1025
DOI 10.1007/s10973-014-4362-6

Study on the molecular structure and thermal stability of pyrimidine nucleoside analogs

Xue-Jie Wang · Jin-Zong You

Received: 13 September 2014 / Accepted: 15 December 2014 / Published online: 29 January 2015

Abstract The thermal decomposition processes for ten pyrimidine nucleoside analogs were measured with thermogravimetry and differential scanning calorimetry. The IR spectra, high-performance liquid chromatography, and liquid chromatography–mass spectrometry of pyrimidine nucleoside analogs and their residues of thermal decomposition at various temperatures were determined. The molecular bond orders of pyrimidines and pyrimidine nucleoside analogs were calculated with an ab initio method from the GAMESS program. We then discuss mechanisms of thermal decomposition in these pyrimidine nucleoside analogs. The results indicate that there are four types of mechanisms. The decomposition mechanism depends on the relative strength of the peptide bond and the amide bond within pyrimidine ring and whether or not accompanied by oxidation reaction. The substituent groups affect the thermal stability and the thermal decomposition mechanism of pyrimidine nucleoside analogs. Increasing the number of electron-donating groups on the pyrimidine ring and furan ring will enhance the peptide bond, and will elevate the temperature of thermal decomposition. There is a positive correlation between the molecular bond orders calculated by quantum chemistry and the thermal decomposition temperature of pyrimidine nucleoside analogs. The stronger the weakest bond order, the higher the decomposition temperature. The molecular bond orders thus can be used as a basis to judge molecular thermal stability for analog compounds with similar molecular structure, size, and energy.

X.-J. Wang (✉) · J.-Z. You
School of Science and Technology, Zhejiang International Studies University, Hangzhou 310012, China
e-mail: xjwang@zisu.edu.cn

Keywords Pyrimidine nucleoside analogs · Thermal analysis · IR spectra · HPLC · LC–MS · Quantum chemistry · Thermal decomposition mechanism

Introduction

Many pyrimidine nucleoside analogs have antiviral activity [1] and anticancer function [2], with some used clinically. For instance, zidovudine (AZT) [3, 4], also known as azido deoxythymidine, or 1-[(2*R*,4*S*,5*S*)-4-azido-5-(hydroxymethyl)oxolan-2-yl]-5-methylpyrimidine-2,4-dione, was approved by the food and drug administration (FDA, USA) in March 1987 [5]. AZT is the world's first FDA-approved human immunodeficiency virus (HIV) drug and is a basic ingredient of "cocktail" therapy. This drug is highly active for retroviruses in vitro including HIV. It is phosphorylated into AZT triphosphate by cell thymidine kinase in the infected cell, and the AZT triphosphate selectively inhibits HIV reverse transcriptase. This stops HIV chain synthesis and thus prevents HIV. AZT may also be used to treat of tumors [6]. Stavudine (d4T) [7–9] (1-((2*R*,5*S*)-5-(hydroxymethyl)-2,5-dihydrofuran-2-yl)-5-methylpyrimidine-2,4(1*H*,3*H*)-dione) is the fourth HIV drug approved by FDA (June 1994) for treatment of HIV infection following AZT, didanosine, and zalcitabine. It inhibits the activity of HIV reverse transcriptase through competition with the natural substrate deoxythymidine triphosphate. This inhibits the extension of DNA, and thus inhibits the replication of HIV in human cells. Lamivudine (3TC) [10–12] (Epivir, 4-amino-1-[(2*R*,5*S*)-2-(hydroxymethyl)-1,3-oxathiolan-5-yl]-1,2-dihydropyrimidin-2-one) is a new nucleoside antiviral drug developed by Canadian Biochem Pharma Company [11]. It was put in the US market by British Glaxo Wellcome Company in 1995 and the UK in

1996 to treat chronic hepatitis B. Telbivudine (LdT) [13, 14] (Sebivo, 1-(2-deoxy-β-L-*erythro*-pentofuranosyl)-5-methylpyrimidine-2,4(1*H*,3*H*)-dione is a new antiviral drug developed by American Idenix Pharmaceuticals Company and produced by the Swiss company Novartis. It was introduced to the Swiss market in September 2006 and inhibits DNA polymerase in hepatitis B. It is used for chronic adult hepatitis B and liver cirrhosis has outcomes superior to 3TC and adefovir dipivoxil.

There are three types of natural pyrimidine compounds: thymine, uracil, and cytosine. In this article, we reported ten pyrimidine nucleoside analogs based on these three pyrimidines. These pyrimidine nucleoside analogs are all composed of two molecular fragments—a pyrimidine ring and a furan ring. These are connected with a peptide bond. The molecular structures of the pyrimidine nucleoside analogs are shown in Scheme 1.

In our previous studies [15–19], we have found that there is high similarity in the thermal decomposition of some nucleoside analogs, but marked differences in others. In this article, the thermal decomposition processes of ten pyrimidine nucleoside analogs under nitrogen atmosphere were studied with thermogravimetric analysis (TG) and differential scanning calorimetry (DSC). The IR spectra, high-performance liquid chromatography (HPLC), and liquid chromatography–mass spectrometry (LC–MS) of pyrimidine nucleoside analogs and their residues of thermal decomposition at different stages were measured. The molecular bond orders of pyrimidine nucleoside analogs were calculated with ab initio methods of quantum chemistry (GAMESS package) [20–23]. Thermal decomposition

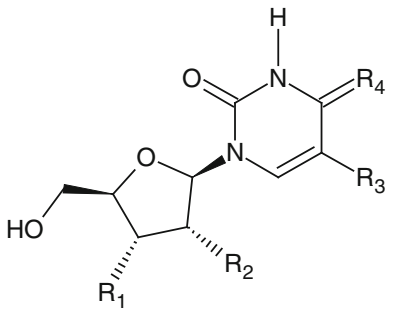

5-Methyluridine: $R_1 = R_1 = -OH$, $R_3 = CH_3$, $R_4 = O$
Thymidine Tebivudine: $R_1 = -OH$, $R_2 = -H$, $R_3 = CH_3$, $R_4 = O$
Zidovudine: $R_1 = -N_3$ $R_2 = -H$ $R_3 = CH_3$, $R_4 = O$
Stavudine: R_1-C-C-R_2 = R_1-C=C-R_2 $R_3 = CH_3$, $R_4 = O$
Uridine: $R_1 = R_1 = -OH$ $R_3 = H$, $R_4 = O$
2′-Deoxyuridine: $R_1 = -OH$ $R_2 = -H$ $R_3 = H$, $R_4 = O$
DTU: C-R_1 = S, $R_2 = -H$, $R_4 = O$
Cytidine: $R_1 = R_1 = -OH$, $R_4 = NH$
Lamivudine: C-R_1 = S, $R_2 = -H$, $R_4 = NH$

Scheme 1 The molecular structure of the pyrimidine nucleoside analogs

mechanisms of pyrimidine nucleoside analogs were discussed and the thermal stability of different analogs could be compared. The relationship between molecular structure and thermal properties of pyrimidine nucleoside analogs was then explored.

Experimental

Reagents

3TC, d4T, LdT, AZT, and 2′-deoxy-3′-thiauridine (DTU) were provided by Hangzhou Coben Pharmaceutical Co., Ltd. The HPLC purities were all over 99 %. Cytidine, cytosine, 2′-deoxyuridine, 5-methyluridine, thymidine, thymine, uracil, and uridine were purchased from Aladdin Industrial Corporation (Shanghai, China) with HPLC purities all over 99 %. Acetonitrile (ACN) (HPLC purity grade) and ammonium acetate (analytical grade) were all purchased from Shanghai Zhanyun Chemical Co., Ltd. (Shanghai, China). Water was produced by a Millipore Elix3 (Billerica, MA, USA) water purifying system.

Measurements and calculations

TG-DTG-DSC simultaneous thermal analysis

The TG, DTG, and DSC curves were obtained with an SDT-Q600 simultaneous thermal analyzer (TA Instruments Inc., USA) under dynamic nitrogen atmosphere (80 mL min^{-1}) at a heating rate of 10.0 °C min^{-1} at the RT-800 °C. The sample masses were 10 mg plus the mass of the alumina ceramic crucible.

Residues of thermal decomposition

The residues of thermal decomposition were prepared in an SDT-Q600 simultaneous thermal analyzer under dynamic nitrogen atmosphere (80 mL min^{-1}) at a heating rate of 10.0 °C min^{-1} from room temperature to defined temperature. Key areas of study included the beginning of mass loss, peak of DTG curve, bottom of the first mass loss step, etc. The sample masses were about 10 mg plus the mass of alumina ceramic crucibles.

IR spectra of solid samples

The IR absorption spectra of samples and residues of thermal decomposition in pressed KBr pellets were obtained with a Nicolet FT-IR spectrophotometer (Model iS 10; Thermo Fisher Scientific Inc. USA) at room temperature. The spectra were collected from 4000 to 400 cm^{-1} with 32 scans and a resolution of 4 cm^{-1}.

HPLC analysis of residues of thermal decomposition

Separation studies of standard samples and residues were performed with an HPLC system from Hitachi High-Technologies Corporation of Japan. The instrument consisted of an LC 2130 quaternary gradient pump with an LC 2140 UV–Vis detector. The data were acquired and processed using HS 2000 chromatography workstation (Hangzhou Science & Techn. Co., China). Reversed phase C-18 columns (250 mm × 4.6 mm i.d. size) containing 5-μm stationery phase were purchased from Shanghai Awence Science & Technology Co., Ltd. The mobile phase was filtered through a 0.45-μm membrane and degassed before use via ultrasonication. The flow rate was kept constant at 1.0 mL min^{-1}, and the temperature of column was maintained at 30 °C. The 5.0-mg of samples (the standard samples or residues of thermal decomposition) were dissolved in 10 mL of mobile phase. A small amount of HAc dilute solution was used to help dissolution. The sample solution was filtered through a 0.45-μm membrane before injection. The injection volume was 5 μL, and detection wavelength was 254 nm.

The mobile phase consisted of 50 mmol L^{-1} ammonium acetate solution as eluent A and ACN as eluent B. The mobile phase gradient for separation of thymidine nucleoside analogs residues was 0–5 min 96 % A and 4 % B; 5–10 min, 92 % A and 8 % B; 10–15 min, 87 % A and 13 % B. The mobile phase gradient for separation of uridine nucleoside analogs residues was 0–4.5 min, 98 % A and 2 % B; 4.5–20 min, 94 % A and 6 % B. The mobile phase gradient for separation of cytidine nucleoside analogs residues was 0–4.5 min, 100 % A; 4.5–20 min, 95 % A and 5 % B.

LC–MS analysis of residues

LC–MS analysis was performed with an HP 1100/LCQ advantage mass spectrometer (Hewlett Packard Company, USA) equipped with an ESI source. The chromatographic separation was carried out on an Acclaim® 120 C18 (4.6 mm × 250 mm × 5 μm). The mobile phase consisted of water as eluent A and methanol as eluent B. The gradient elution used started with 5 % B which was maintained at 2 min, then programmed to increase % B to 20 % in 10 min, the mobile phase was maintained at 20 % B until 5 min after which % B was decreased back to starting point of 5 %, where it was maintained until 15 min before the start of the next run. The flow rate was 1.0 mL min^{-1}, and the temperature of column was maintained at 25 °C. Mass spectra were acquired in both negative and positive modes with ion spray voltage at 4.50 kV, capillary temperature at 280 °C, capillary voltage at 19 V, sheath gas flow at 30 (arbitrary units), auxiliary gas at 10 (arbitrary units), and tube lens offset at 25 V. About 10 mg of sample (residue of thermal decomposition) was dissolved in 5 mL of mobile phase. The sample solution was filtered through a 0.45-μm membrane before injection. The injection volume was 10 μL.

Quantum chemical methods

The molecular structures of pyrimidine and pyrimidine nucleoside analogs were drawn with ChemDraw software in ChemOffice, and optimized with a MM2 dynamics method. The molecular energy, charge distribution, and bond order were calculated with the GAMESS program—a general ab initio quantum chemistry package attached to ChemDraw. Program parameters include Job Type: Minimize [energy/geometry]; Method: HF; Basis Set: 3-21G; Wave Function: R-Closed-Shell; Polarization: None; Diffuse: None; Exponent: POPLE; Opt. Algorithm: QA; and Move Which: All Atoms. The program default values were adopted for the computational accuracy and convergence threshold; all calculations were completed on a personal computer.

Results and discussion

Thermal decomposition processes of pyrimidine nucleoside analogs

Figure 1 presents the thermal decomposition curves of three pyrimidines and ten pyrimidine nucleoside analogs under nitrogen atmosphere.

The thymidine nucleoside analogs have two or more peaks on their DTG curves except for 5-methyluridine (Fig. 1). This suggests that there are two or more steps in these decomposition processes. The temperatures of the first DTG peaks are different from one another for thymidine, LdT, d4T, and AZT, but the temperatures of their second DTG peaks are very close to each other, they are 303.7, 306.9, 303.0, and 298.5 °C, respectively. The DTG peak temperature of 5-methyluridine is 305.1 °C. All are similar to the DTG peak temperature of thymine (319.3 °C). These results suggest that this stage (the second mass loss steps) all are the decomposition of thymine ring, and the thermal decomposition of thymidine nucleoside analogs all progress through the thymine stage.

There is a large space between two DTG peaks of d4T and two clear mass loss steps. The mass loss rate of the first steps is 21.2 %, clearly lower than the theoretical value from lost furan ring (44.15 %). This may imply a polymerized double bond in dihydrofuran during the first stage. While there are small spaces between the two DTG peaks of thymidine, LdT and AZT, as well as unclear

demarcation for the two mass loss steps. LdT is the L-enantiomer of thymidine, and their thermal analysis curves are almost exactly the same. This means that their thermal decomposition processes are the same. The mass loss rates at the inflection point of the TG curve for LdT and thymidine are 58.2 and 56.0 %, respectively. This is slightly larger than the theoretical value of furan loss (48.3 %). The mass loss rate of the first mass loss steps of AZT is 28.4 %, much lower than the theoretical value of furan loss (53.2 %). These data indicate that the first stages of thermal decomposition of thymidine nucleoside analogs are not only a simple fracture of the peptide bond, but that pyrolysis of the thymine rings is continuous or partially synchronous phenomenon.

In uridine nucleoside analogs, the thermal analytical curves of uridine and DTU are similar. Their TG curves both show one big fast mass loss steps and followed by a slow process of mass loss. Their DTG peak temperatures are 291.1 and 294.4 °C, respectively, both are slightly lower than that of uracil (337.0 °C), but their peak width is larger than that of uracil and covers the decomposition temperature range of uracil. This means that the thermal decomposition of uridine and DTU both are synchronous or continuous decomposition processes and that the

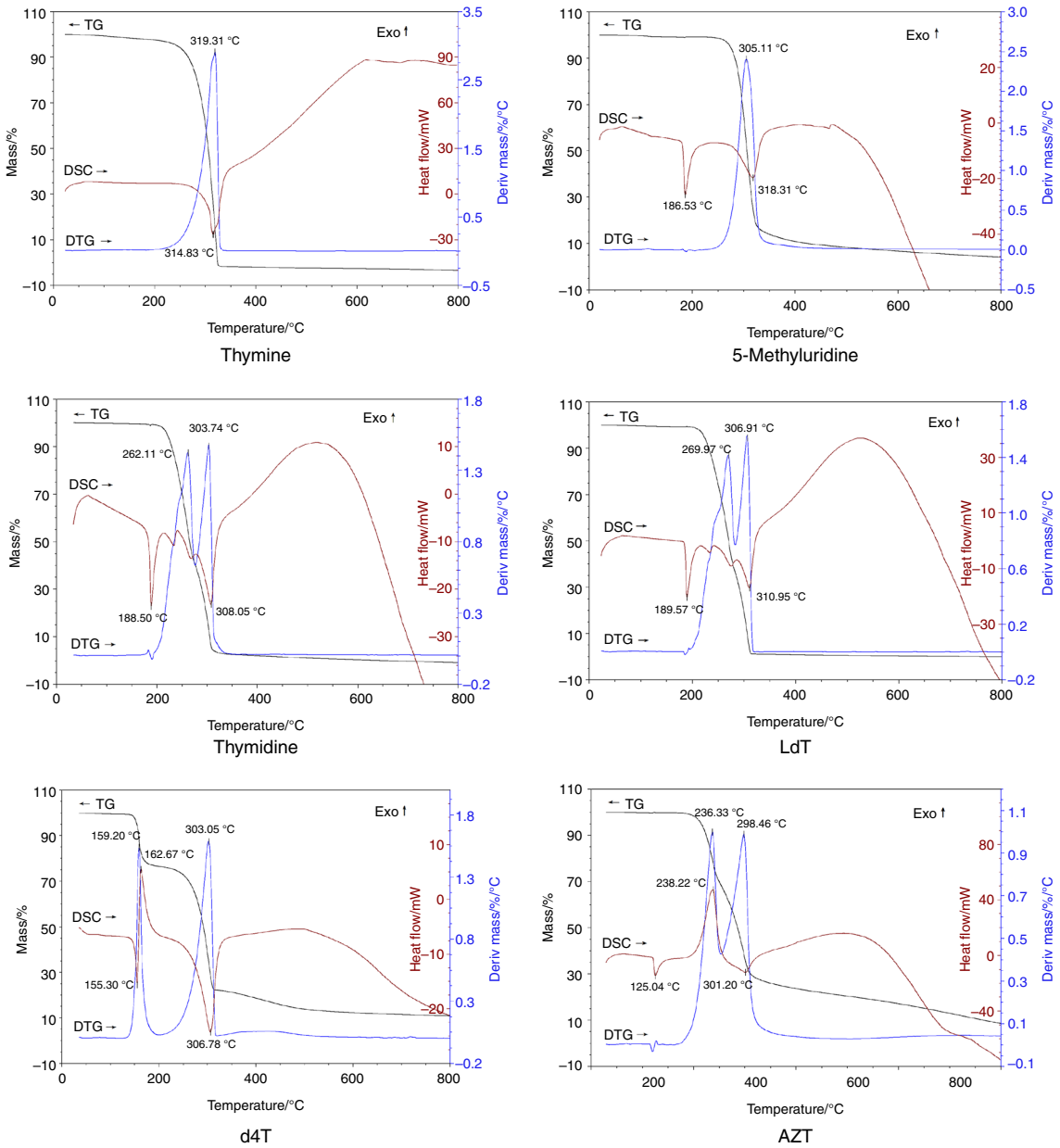

Fig. 1 TG, DTG, and DSC curves of pyrimidines and pyrimidine nucleoside analogs under nitrogen atmosphere, heating rate: 10 °C min^{-1}

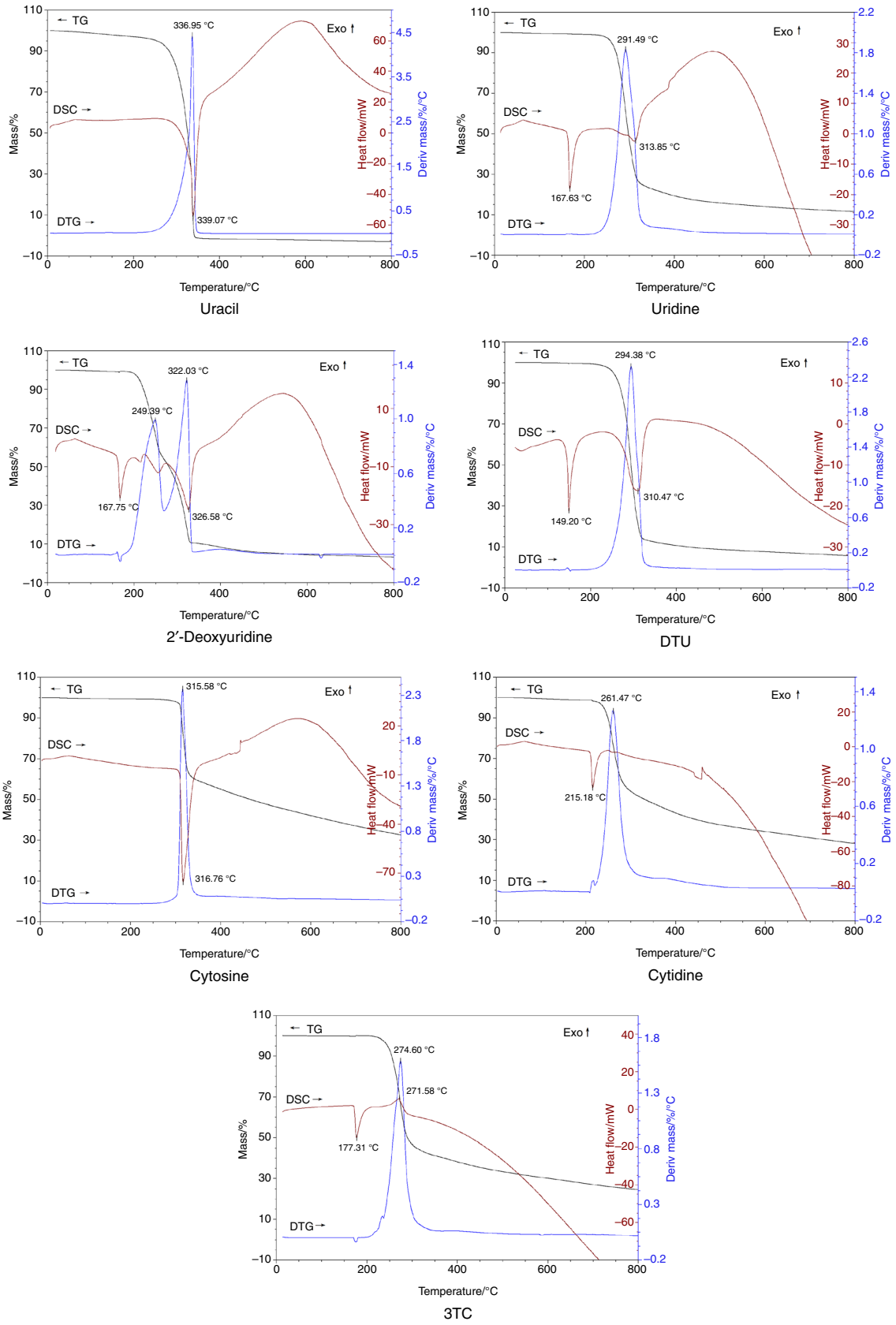

Fig. 1 continued

decomposition of the uracil ring occurs in this step. There are two peaks on the DTG curve of 2′-deoxyuridine. The second DTG peak temperature is 322.08 °C, close to that of uracil (337.0 °C). There is no clear demarcation for these two mass loss steps. The mass loss rate of the first mass loss step is 42.2 %, and slightly lower than the theoretical value of a furan loss (51.3 %). It indicates that the thermal decomposition of 2′-deoxyuridine may go through the uracil stage, and it also is a partial synchronous decomposition process.

In cytidine nucleoside analogs, the thermal analytical curves of cytidine and 3TC are similar. Their TG curves both show one big fast mass loss steps and followed by a slow process of mass loss. Their DTG peak temperatures are 261.5 and 274.6 °C, respectively. They both are considerably lower than cytosine (315.6 °C). This means that the thermal decomposition of cytidine and 3TC both are synchronous decomposition processes.

The DSC curves of 5-methyluridine, thymidine, LdT, AZT, uridine, 2′-deoxyuridine, DTU, cytidine, and 3TC all show a sharpened endothermic melting peak at 186.5, 188.5, 189.6, 125.0, 167.6, 167.8, 149.2, 215.2, and 177.3 °C, respectively, before the mass loss. The DSC curve of d4T shows a sharpened endothermic peak at the beginning of the decomposition, it means d4T melts at the beginning of the decomposition. The DSC curves of thymine, uracil, and cytosine all have large endothermic peaks suggesting that the thermal decomposition processes of these pyrimidines in nitrogen are all thermal cracking processes. The DSC curves corresponding to the first mass loss stage of pyrimidine nucleoside analogs are all exothermic peaks or smaller endothermic peaks except for 5-methyluridine and DTU. This suggests that the first stage of thermal decomposition, namely the decomposition of multi-hydroxyl furan ring, contains oxidation reactions. The DSC curves of decomposition processes for 5-methyluridine and DTU and the DSC curves corresponding to the second mass loss stage of other pyrimidine nucleoside analogs are all endothermic peaks. This suggests that these stages, namely the decomposition of pyrimidine rings, are thermal cracking processes.

IR spectroscopic analysis of intermediate residues for the thermal decomposition of pyrimidine nucleoside analogs

The analysis of solid residues formed at various temperatures can also provide direct information on the changes that occur in the chemical composition of organic samples during thermal degradation. The IR spectra of pyrimidine nucleoside analogs and their residues from various stages of thermal decomposition were measured.

Figure 2 presents the IR spectra of thymine and residues of thermal decomposition of various thymidine nucleoside analogs obtained at the bottom of the first stage (near the DTG peak of 5-methyluridine). The IR spectra of intermediate products of various thymidine nucleoside analogs are all very consistent with thymine. This suggests that the major ingredient of these residues is thymine and that the thermal decomposition processes of thymidine nucleoside analogs all go through the thymine stage. The first step in thermal decomposition of these thymidine analogs is fracture of the peptide bond.

Figure 3 presents the IR spectra of uracil and residues of uridine nucleoside analogs during thermal decomposition. The IR spectrum of uridine residue obtained near the DTG peak (290 °C, about 33 % mass loss), the IR spectrum of 2′-deoxyuridine residue obtained at the bottom of the first mass loss step (255 °C), and the IR spectrum of DTU residue obtained at 285 °C (mass loss step 30 %) are consistent with the IR spectrum of uracil. This means that main parts of the residues are uracil, and the thermal decomposition processes of uridine, 2′-deoxyuridine, and DTU all undergo through uracil stage. The difference between the IR spectra of residues with the IR spectrum of uracil indicates that the residues contain other decomposition products. The differences between the IR spectra of uridine residue versus that of uracil are obvious relatively—the uridine residue contains more other decomposition products.

Figure 4 shows the IR spectra of intermediate residues of the thermal decomposition of cytidine nucleoside analogs. We can find that the IR spectrum of cytidine residue

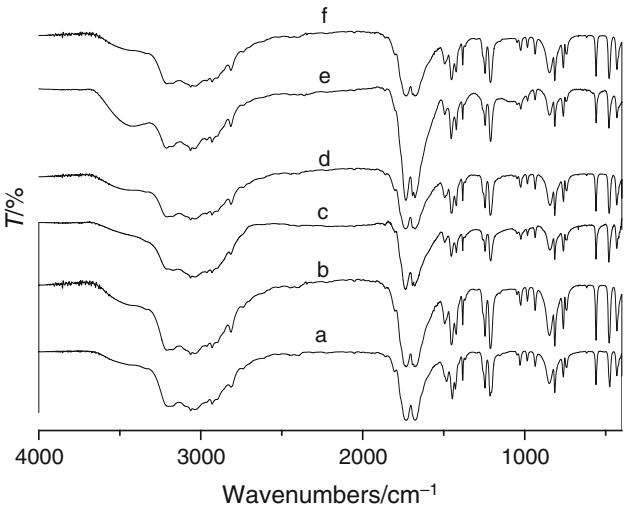

Fig. 2 IR spectra of residues of thymidine nucleoside analogs in thermal decomposition. *a* Thymine, *b* residue of thymidine obtained at 260 °C, *c* residue of LdT obtained at 260 °C, *d* residue of AZT obtained at 240 °C, *e* residue of d4T obtained at 170 °C, and *f* residue of 5-methyluridine obtained at 300 °C

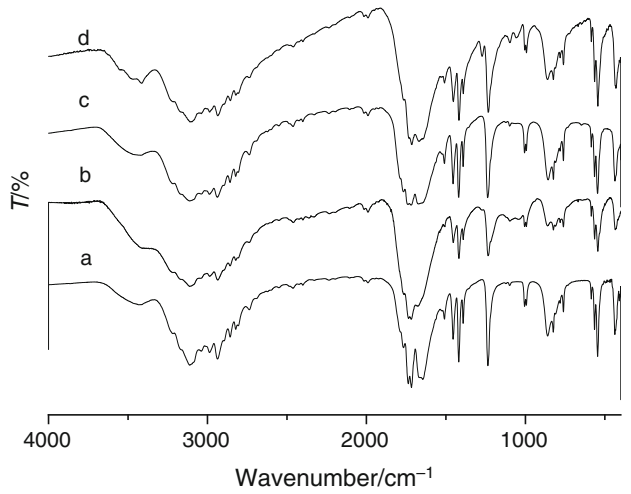

Fig. 3 IR spectra of residues of uridine nucleoside analogs in thermal decomposition. *a* Uracil, *b* residue of uridine obtained at 290 °C, *c* residue of 2′-deoxyuridine obtained at 255 °C, and *d* residue of DTU obtained at 285 °C

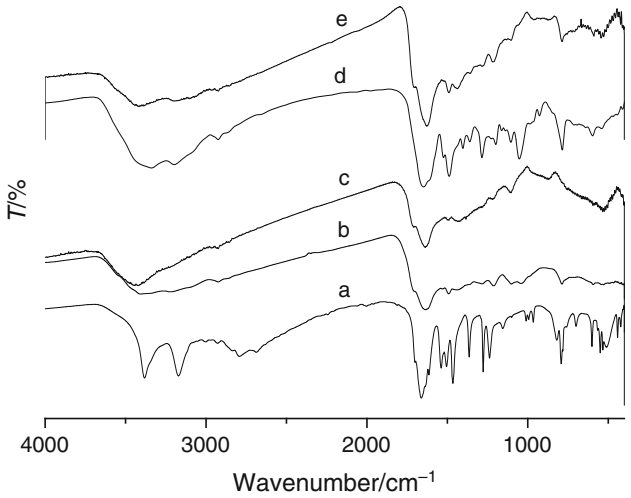

Fig. 4 IR spectra of residues of cytidine nucleoside analogs during thermal decomposition. *a* Cytosine, *b* residue of cytidine obtained at 245 °C, *c* residue of cytidine obtained at 270 °C, *d* residue of 3TC obtained at 255 °C, and *e* residue of 3TC obtained at 265 °C

obtained at 245 °C (about 10 % mass loss) and the IR spectrum of 3TC residue obtained at 255 °C (about 10 % mass loss) both have obvious change compared with cytidine and 3TC, and both are clearly different from the IR spectrum of cytosine. But two IR spectra both have the C–OH peak (1053 cm^{-1}) and the C–O–C peak (1102 cm^{-1}). It means that part of cytidine and 3TC has not yet decomposed at this time. The IR spectrum of cytidine residue obtained at 270 °C (about 35 % mass loss) and the IR spectrum of 3TC residue obtained at 265 °C (about 42 % mass loss) both show that most of molecular structures have been destroyed at this temperature and two IR spectra are remarkably similar to each other. It means that the final decomposition product of cytidine and 3TC is same at this stage. These results imply that the decomposition of most of cytidine and 3TC do not undergo through cytosine stage.

HPLC analysis on intermediate residues of pyrimidine nucleoside analogs

In order to know whether the thermal decomposition of pyrimidine nucleoside analogs go through corresponding pyrimidine stages, the intermediate residues of thermal decomposition were analyzed with HPLC and compared to the chromatograms of standard samples (Figs. 5, 6, 7).

Figure 5 presents HPLC chromatograms of thermal decomposition residues of various thymidine nucleoside analogs obtained at the bottom of the first stage (near the DTG peak for 5-methyluridine). The residue of 5-methyluridine obtained at 300 °C is a black solid. Parts of it can be dissolved in acidic water and turn into a colorless solution. There is some insoluble black precipitate (All insoluble precipitate in this paper are insoluble in water and insoluble in organic solvents). The residues of thymidine and telbivudine obtained at 260 °C both are a gray–white solid; most of them can be dissolved into acidic water and turn into a colorless solution, but there is a small amount of insoluble brown precipitate. The residue of d4T obtained at 170 °C is a white solid that can be completely dissolved

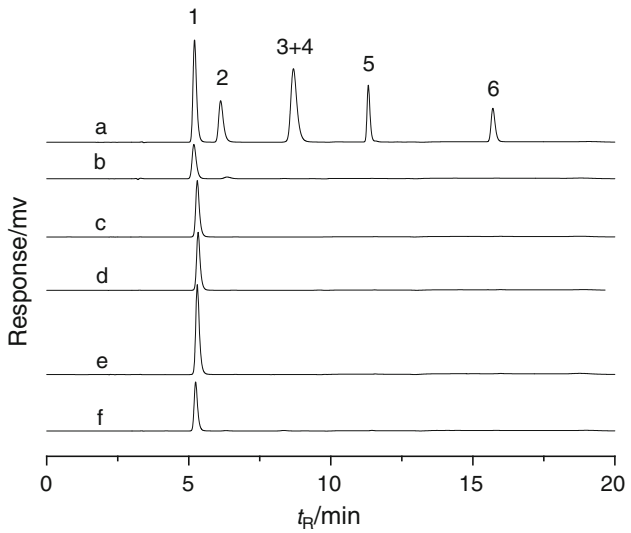

Fig. 5 HPLC chromatograms of thymidine nucleoside analogs residues from thermal decomposition. *a* Standard samples (every one 5 mg mL^{-1}): *1* thymine, *2* 5-methyluridine, *3* thymidine, *4* LdT, *5* d4T, and *6* AZT. *b* Residue of 5-methyuridine formed at 300 °C. *c* Residue of thymidine formed at 260 °C. *d* Residue of LdT formed at 260 °C. *e* Residue of d4T formed at 170 °C. *f* Residue of AZT formed at 240 °C

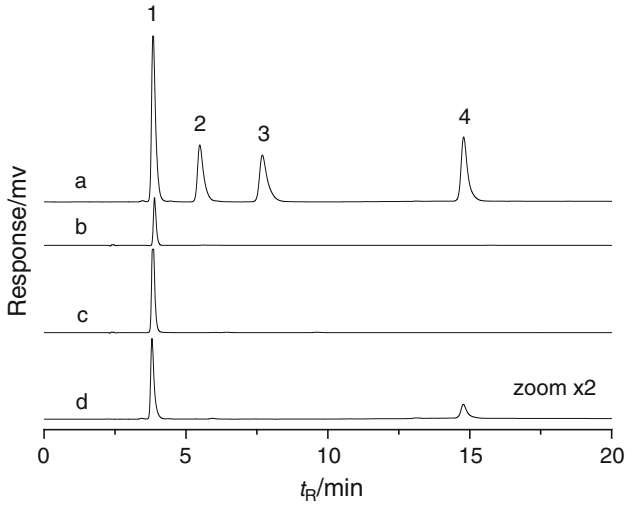

Fig. 6 HPLC chromatograms of uridine nucleoside analogs residues from thermal decomposition. *a* Standard samples (every one 5 mg mL^{-1}): *1* uracil, *2* uridine, *3* 2′-deoxyuridine, and *4* DTU. *b* Residue of uridine formed at 290 °C. *c* Residue of 2′-deoxyuridine formed at 255 °C. *d* Residue of DTU formed at 285 °C

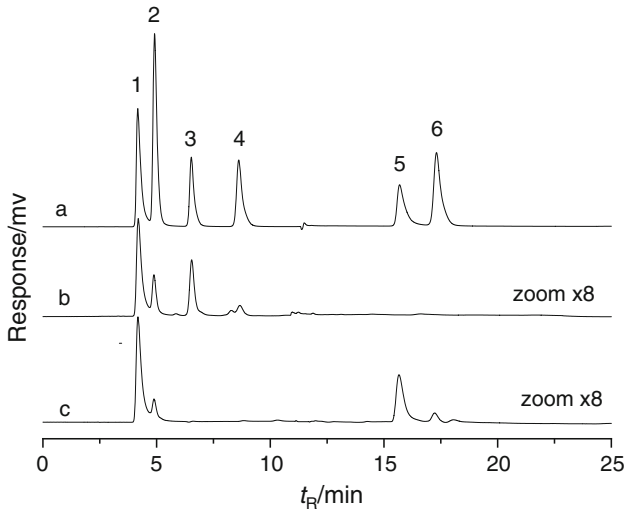

Fig. 7 HPLC chromatograms of cytidine nucleoside analogs residues from thermal decomposition. *a* Standard samples (every one 5 mg mL^{-1}): *1* cytosine, *2* uracil, *3* cytidine, *4* uridine, *5* 3TC, and *6* DTU. *b* Residue of cytidine formed at 245 °C. *c* Residue of 3TC formed at 250 °C

into the mobile phase and turn into a colorless solution. The residue of AZT obtained at 240 °C is black spumescent solid; part of it can be dissolved into the mobile phase and turn into a colorless solution, and there is some black insoluble precipitate.

We can see from Fig. 5 that there is only one thymine peak in the HPLC chromatograms for thymidine nucleoside analogs residues. This implies that most of the soluble substances in these residues are thymine (the furan fragment cannot be detected by the UV–Vis detector). The thermal decomposition processes of the thymidine nucleoside analogs all go through the thymine stage. The insoluble precipitates suggest that there is a part of thymine and thymidine nucleoside analogs pyrolyze and carbonize to form insoluble substance at this stage. The onset temperatures of 5-methyluridine and AZT both are higher—there are more thymine rings to synchronously pyrolyze and carbonize. Therefore, their residues contain more insoluble substance and lesser thymine. By comparison, the onset temperature of d4T is lower. There are few thymine rings to pyrolyze synchronously, and its residue contains much more thymine and don't contain insoluble substances.

Figure 6 presents the HPLC chromatograms of thermal decomposition residues of uridine nucleoside analogs obtained at near the DTG peak (or the bottom of the first stage for 2′-deoxyuridine). The residue of uridine obtained at 290 °C (mass loss about 33 %) is a black solid, it is only partially soluble in mobile phase and form a nearly colorless solution. There is some black insoluble precipitate. The residue of 2′-deoxyuridine obtained at 255 °C (mass loss about 61 %) is a light brown solid, most of it can be dissolved into mobile phase and turn into a nearly colorless solution, and there is some insoluble brown precipitate. The residue of DTU obtained at 285 °C (mass loss about 30 %) is a black solid, it is only partially soluble in mobile phase and form a nearly colorless solution. There is some black insoluble precipitate. From Fig. 6, we can see that there are only uracil peak in the HPLC chromatograms of uridine nucleoside analogs residues (except for small DTU peak in DTU's HPLC). This means that most of the soluble substances in the residues are uracil, and that the thermal decomposition processes of uridine nucleoside analogs go through the uracil stage. The insoluble precipitate indicates that a part of uridine nucleoside analogs pyrolyzes and carbonizes directly. The smaller uracil peaks and much more insoluble precipitate indicate that much more uridine and DTU pyrolyze and carbonize directly.

Figure 7 presents the HPLC chromatograms of cytidine nucleoside analogs residues from thermal decomposition. The standard samples of cytosine, uracale, cytidine, uridine, 3TC, and DTU are dissolved in mobile phase and turn into a colorless solution, and their retention times are 4.28, 4.91, 6.53, 8.62,15.69, and 17.30 min, respectively. The cytidine residue obtained at 245 °C is a black solid. A part of it can be dissolved into mobile phase and turn into a nearly colorless solution with some black insoluble precipitate. Compared with the HPLC chromatogram of standard samples, we can see that there are small peaks of cytosine and cytidine, and smaller peaks of uracil and uridine in the chromatogram of this residue. The residue of 3TC obtained at 250 °C is a black spumescent solid

partially soluble in mobile phase to form a slight yellow solution. There is some black insoluble precipitate. There are small peaks of cytosine and 3TC, and smaller peaks of uracil and DTU in the chromatogram of this residue. These very small peaks and insoluble precipitate indicate that most of cytidine and 3TC decompose and carbonizes directly to form insoluble substance and small molecules. The small peak of cytosine implies that a few of cytidine and 3TC go through cytosine stage during the decomposition. The uracil, uridine, and DTU peaks indicate that there is intermolecular oxidation reaction occurrence during the decomposition, a part of cytidine is oxidized to uridine, a part of 3TC is oxidized to DTU, and a part of cytosine is oxidized to uracil, or some uridine, and DTU decompose to uracil.

LC–MS analysis on intermediate residues of pyrimidine nucleoside analogs

In order to confirm the composition of the residues of cytidine and 3TC, the soluble fraction of the residues formed at initial stage of thermal decomposition of cytidine (245 °C) and 3TC (250 °C) was analyzed with LC–MS method, and the results show in Figs. 8 and 9, respectively.

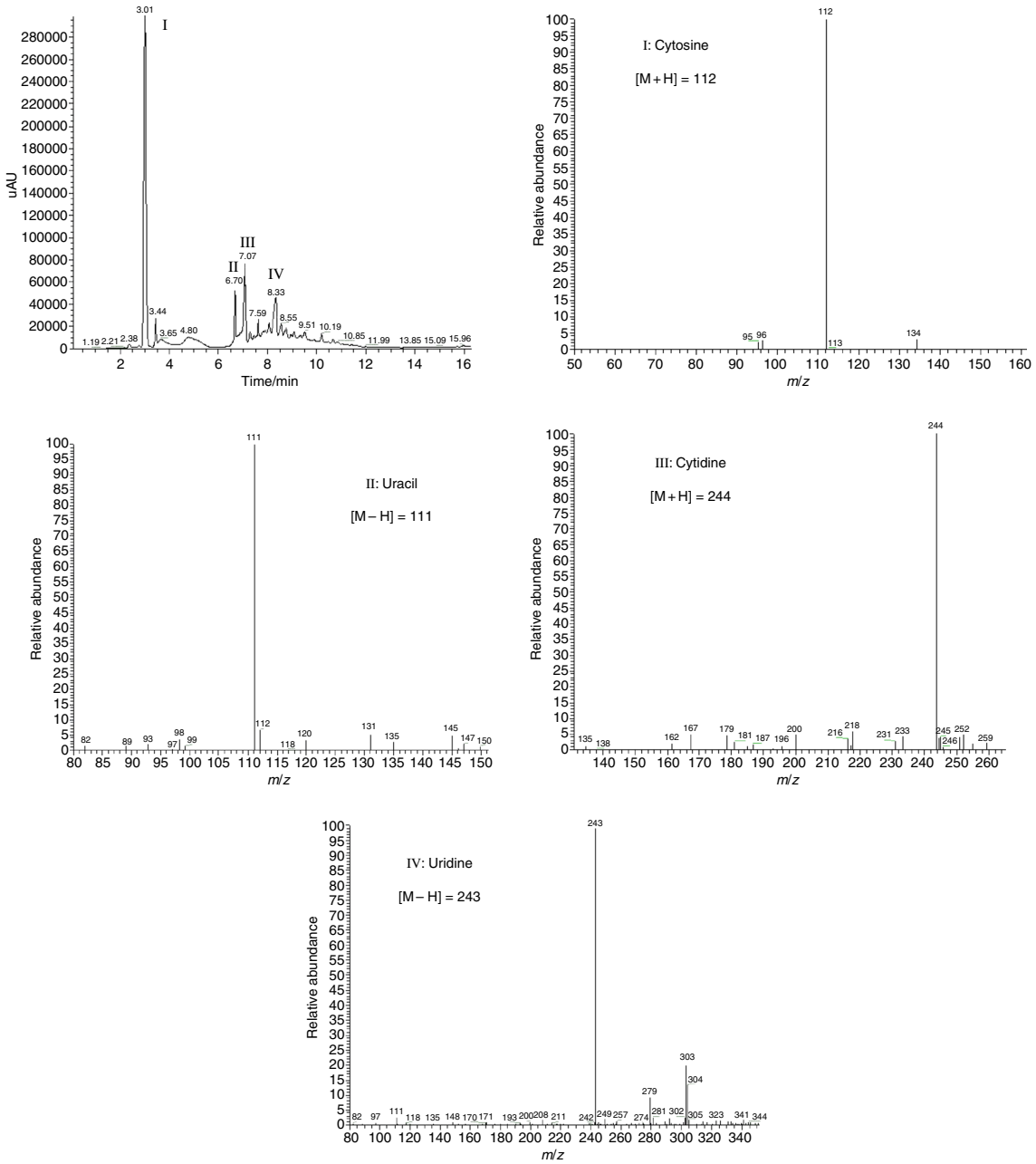

Fig. 8 LC–MS results of cytidine residue obtained at 245 °C

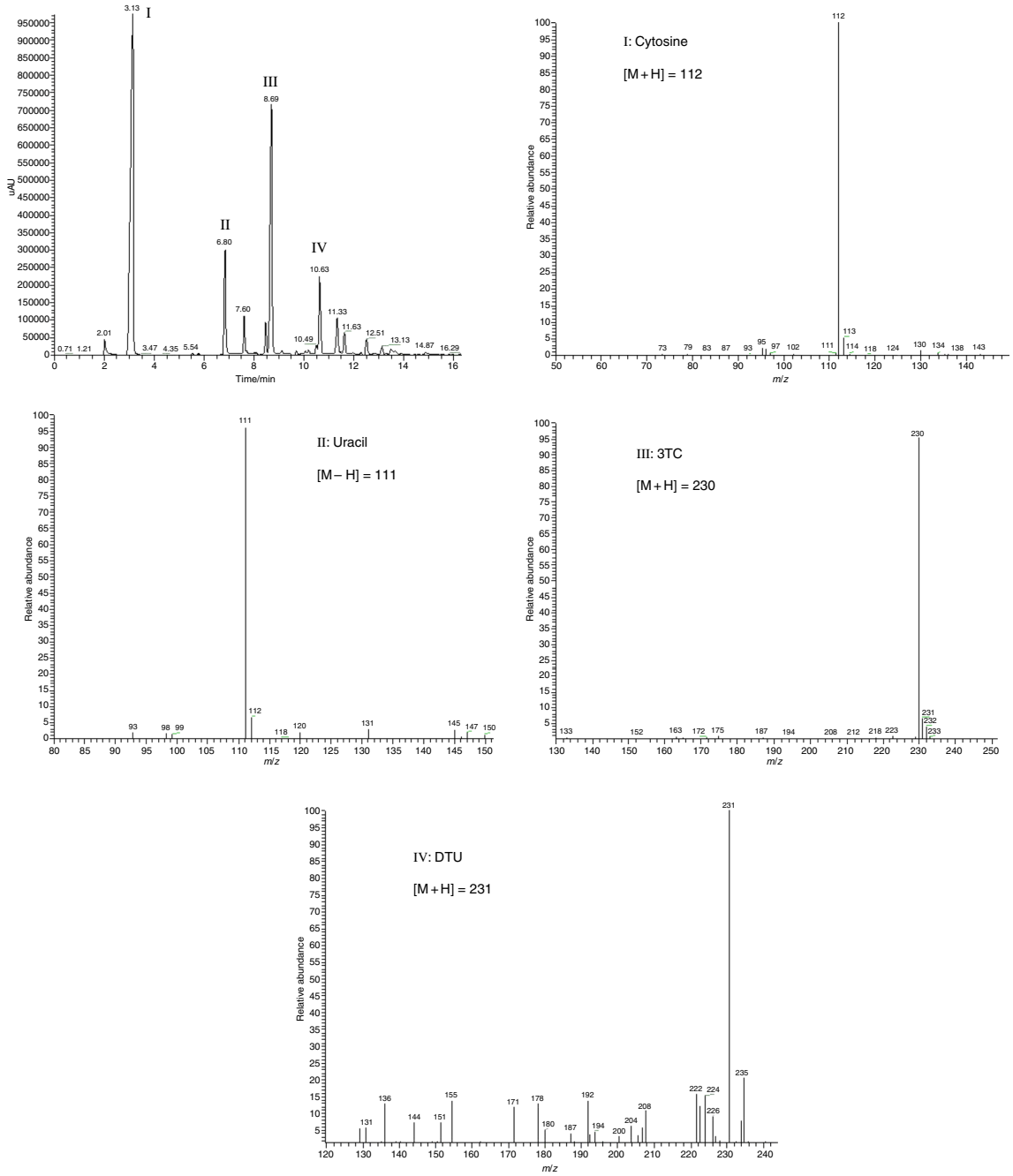

Fig. 9 LC–MS results of 3TC residue obtained at 250 °C

The results of LC–MS confirm the results of HPLC. The residue of cytidine contains cytosine, uridine, and uracil. The residue of 3TC contains cytosine, uracil, and DTU.

Quantum chemical calculation of pyrimidine nucleoside analogs

We discuss the thermal decomposition mechanisms of pyrimidine nucleoside analogs from the perspective of molecular structure, although there are many factors affecting the molecular thermal stability including molecular bond order [24], configuration and total energy, activation energy [25], transition state stability [26], heating rate, etc. Theoretically, the thermal decomposition process of organic molecules is the result of increased molecular kinetic energy and the breaking of chemical bond due to heating. This kinetic energy is due to the aggravation of atomic oscillation. Molecular bond

order can be used as simple criterion of thermal stability for analog compounds with similar molecular structure, size, and energy. Lower the chemical bond order offers easier fracture.

The molecular bond order distribution of pyrimidine and pyrimidine nucleoside analogs was calculated with quantum chemistry ab initio method using the GAMESS program (Scheme 2). According to the molecular bond order

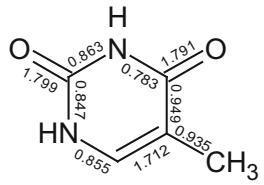

Thymine

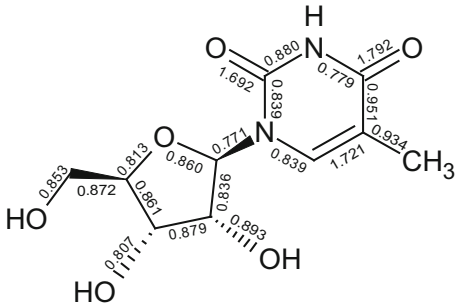

5-Methyluridine

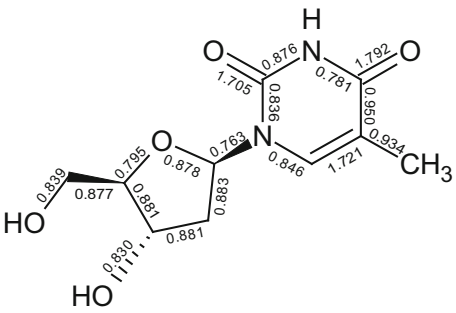

Thymidine

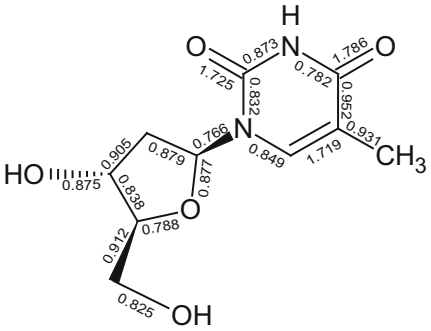

LdT

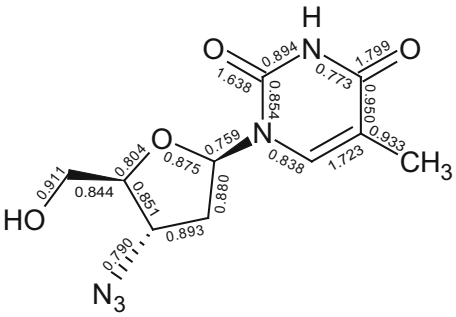

AZT

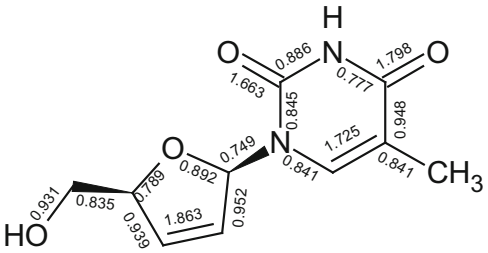

d4T

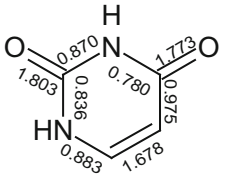

Uracil

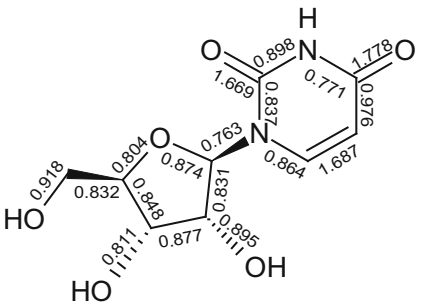

Uridine

Scheme 2 The molecular bond orders of pyrimidine nucleoside analogs

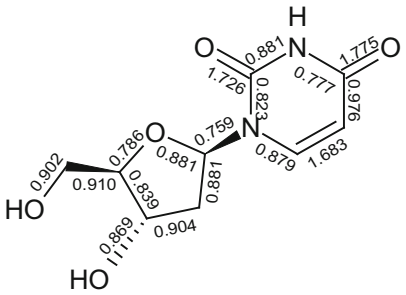

2′-Deoxyuridine

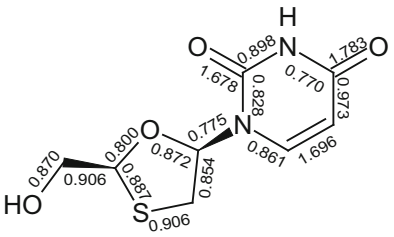

DTU

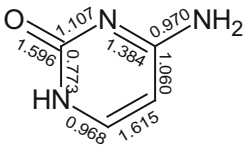

Total energy -390.4162

Cytosine(keto form)

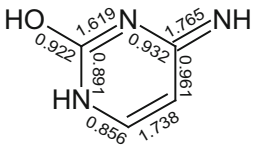

Total energy -390.3715

Cytosine(enol form)

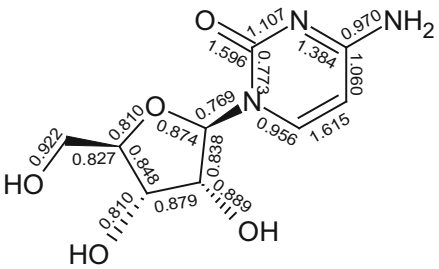

Cytidine

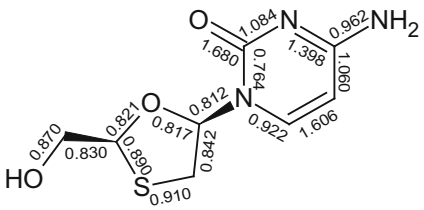

3TC

Scheme 2 continued

distribution of pyrimidine nucleoside analogs, we can judge the location and sequence of molecular bond fracture, and therefore speculate the thermal decomposition mechanisms of pyrimidine nucleoside analogs.

We can see from Scheme 2 that the weakest molecular bonds in the five thymidine nucleoside analogs all are the peptide bond, it will fracture first to form thymine and furan ring intermediate during the thermal decomposition. The thymine is relatively stable and furan ring is unstable because of many weak bonds and active multi-hydroxyl groups. So, the furan ring intermediate will decompose fast to form the first mass loss step. Because the difference between the peptide bond orders of thymidine, LdT, and AZT (0.763, 0.766, and 0.759, respectively) and the weakest bond orders within the pyrimidine ring (0.781, 0.782, and 0.773, respectively) is not big enough, a part of nucleoside will decompose synchronously during this stage. So, their TG curve piecewise lines are not clear, the spaces between two DTG peaks are relatively small, and the residues of thermal decomposition from this stage contain some insoluble precipitate. The peptide bond order of 5-methyluridine is bigger (0.771) and closer to the weakest bond within the pyrimidine ring (0.779). Thus, the initial decomposition temperature of 5-methyluridine is higher, and its pyrimidine ring pyrolysis follows closely. Its DTG curve shows a single peak of continuous decomposition. Its residue of thermal decomposition contains more insoluble precipitate and lesser thymine. The peptide bond order of d4T is the lowest (0.749) and notably smaller than the weakest bond order within the pyrimidine ring (0.777). Thus, the initial decomposition temperature of d4T is the lowest. Furthermore, the pyrimidine ring is pyrolyzed after a while, its TG curve shows two clear mass loss steps, and its DTG curve shows two peaks that are mostly resolved. Its residue of thermal decomposition contains more thymine and don't contain insoluble precipitate.

The weakest bonds of uridine and 2′-deoxyuridine both are the peptide bonds, but the peptide bond order of

2′-deoxyuridine (0.759) is observably less than the weakest bond within the pyrimidine ring (0.777). Therefore, the DTG curve of 2′-deoxyuridine has two peaks, the mass loss of the first stage is close to that predicted by theory, and the residue of the first stage contains more uracil and fewer insoluble precipitate. The weakest bond of DTU is the C–N bond of amide (0.770) within the pyrimidine ring, but the peptide bond orders of uridine (0.763) and DTU (0.775) both are quite close to the weakest bonds within their pyrimidine ring (0.771, 770). Therefore, their thermal decomposition processes are similar as the case of 5-methyluridine. The fracture of the peptide bond and the pyrolysis of the uracil ring occur nearly synchronous. Their DTG curves show a single peak of continuous decomposition, and their residues of thermal decomposition both contain fewer uracil and more insoluble precipitate.

Cytosine can have keto or enol forms [27, 28]. The calculation of quantum chemistry indicates that the total energy of the keto form cytosine is −390.4162 (eV), and is slightly lower than that of the enol form cytosine (−390.3715 eV). It means that the keto form cytosine is more stable structure. The weakest bond order of cytosine with the keto form is the C–N bond (0.773) of amide within the pyrimidine ring. The weakest bond of cytosine with the enol form is the C–N bond (0.856) of cyclamine. Contrasted with the decomposition temperature of cytosine (310.5 °C), we think that the keto form is a relatively reasonable structure. The weakest bond of cytidine is the peptide bond (0.769), but the amide C–N bond within the pyrimidine ring is also same weak (0.773). Therefore, the fracture of the peptide bond and the pyrolysis of the pyrimidine ring are nearly simultaneous during thermal decomposition with a single peak in the DTG. The weakest bond of 3TC is the C–N bond (0.764) of the amide within the pyrimidine ring, and this bond order is much low than that of the peptide bond (0.812). Therefore, the pyrimidine ring of 3TC will be pyrolyzed first during thermal decomposition. So, its residue of thermal decomposition contains more insoluble and lesser cytosine. The furan ring and 1,3-oxathiolane ring are easy to decompose and to form free oxygen, the amino group in cytosine ring is easy to be oxidized and to form hydroxyl group or carboxide group. This oxidation reaction makes 3TC be translated into DTU, cytidine be translated into uridine, and cytosine be translated into uracil. The generated uridine, DTU, and uracil will decompose as the models of uridine, DTU, and uracil, respectively. So, the residues of cytidine contain small amount of uridine, cytosine, and urical. The residues of 3TC contain small amount of DTU, cytosine, and uracil.

Because the peptide bond orders are close to the weakest bonds within the pyrimidine, the decomposition of some pyrimidine nucleoside analogs is continuous or synchronous processes, and there are large differences between their actual mass loss of the first stage and the theoretical mass loss.

Because of weak C–O bonds and the oxidative decomposition of furan ring and 1,3-oxathiolane ring, the DSC curves of the first stage of pyrimidine nucleoside analogs all have exothermic peak or small endothermic peak. The thermal pyrolysis of the pyrimidine ring is mostly due to bond fracture under higher temperature, and the DSC curves have an endothermic peak.

Discussion on thermal decomposition mechanisms of pyrimidine nucleoside analogs

Based on the above research, we infer that there are four mechanisms for the thermal decomposition of pyrimidine nucleoside analogs studied in this article (Scheme 3).

The decomposition mechanism depends on the relative strength of the peptide bond and the amide bond within pyrimidine ring and whether or not there is oxidation reaction. When the peptide bond order is observably lower than that of the weakest bond within pyrimidine ring, the decomposition mechanism will be according to mechanism 1, such as thymidine, LdT, AZT, d4T, and 2′-deoxyuridine. When the peptide bond order is close to that of the weakest bond within pyrimidine ring, the decomposition mechanism will be according to mechanism 2, for example 5-methyluridine, uridine, and DTU. When the peptide bond order is close to that of the weakest bond within pyrimidine ring, and there is oxidation reaction. The decomposition mechanism will be according to mechanism 3, for example cytidine. When the peptide bond order is observably larger than that of the weakest bond in pyrimidine ring, and there is oxidation reaction. The decomposition mechanism will be according to mechanism 4, the pyrimidine ring is pyrolyzed first, for example 3TC.

Effect of substituents on molecular stability of pyrimidine nucleoside analogs

The differences in thermal stability and decomposition mechanism of pyrimidine nucleoside analogs are related to molecular structure. Increasing electron-donating groups on pyrimidine or furan ring will increase charge density of the ring, strengthen the peptide bond order, and will rise the decomposition temperature. Conversely, the peptide bond order will be weakened and the decomposition temperature will be decreased. Quantum chemical calculations confirm this. For example, the peptide bond orders of all deoxyribonucleosides are less than their corresponding nucleosides, and the decomposition temperatures of all deoxyribonucleosides are lower than their corresponding nucleosides. Versus thymidine nucleoside analogs, the

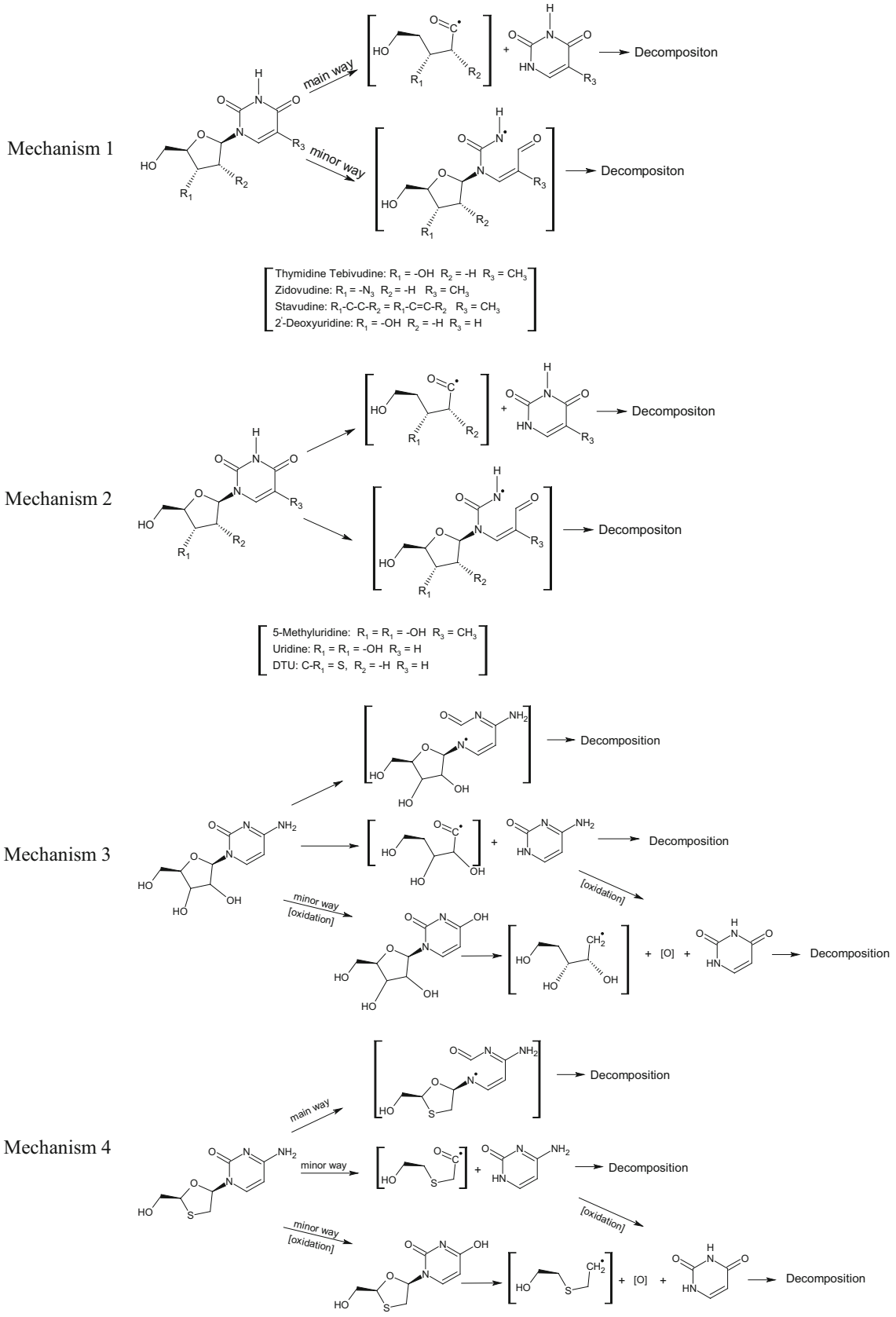

Scheme 3 Postulated mechanisms of thermal decomposition for pyrimidine nucleoside analogs

Table 1 Temperature of decomposition including onset point, temperature of DTG peak, and weakest bond orders of pyrimidine nucleoside compounds

Compounds	Temperature of decomposition (onset point)/°C	Temperature of DTG peak/°C	Weakest bond orders
Thymine	283.4	318.8	0.783
5-Methyluridine	285.3	305.0	0.771
Thymidine	223.9	261.2	0.763
LdT	225.5	267.3	0.766
d4T	154.1	159.3	0.749
AZT	213.6	236.0	0.759
Uracil	308.4	336.9	0.780
Uridine	271.4	291.5	0.763
2′-Deoxyuridine	212.1	249.2	0.759
DTU	263.5	294.4	0.770
Cytosine	310.5	315.7	0.773
Cytidine	243.8	260.3	0.769
3TC	250.7	274.5	0.764

pyrimidine rings of uridine nucleoside analogs lack one electron-donating methyl group. The charge density within the ring is decreased and the peptide bond order is weakened. Therefore, the thermal decomposition temperatures of uridine nucleoside analogs are lower than the corresponding thymidine nucleoside analogs. Versus 5-methyluridine, the furan rings of thymidine and LdT are reduced by an electron-donating hydroxyl group. Therefore, the decomposition temperatures of thymidine and LdT are lower than that of 5-methyluridine. There is only one hydroxyl group in the furan ring of AZT, and the electron-donating property of the azido is lower than that of the hydroxyl group. Thus, the decomposition temperature of AZT is slightly lower than that of thymidine. The furan ring of d4T lacks one hydroxyl group versus thymidine. The C=C bond is electron withdrawing, and the decomposition temperature of d4T is much lower than that of thymidine. One carbon atom is substituted by an electron-donating sulfur within the furan ring of DTU, the peptide bond orders of DTU are greater than uridine, and the decomposition temperature of DTU is higher than uridine. Versus uridine, the electron-withdrawing aldehyde group is substituted by an electron-donating amino group at pyrimidine ring of cytidine, the peptide bond orders of cytidine are greater than uridine, and the decomposition temperature of cytidine is higher than uridine. The electron-donating 1,3-oxathiolane ring makes the peptide bond order of 3TC greater than cytidine. But, the peptide bond order also larger than the weakest bond within pyrimidine ring of 3TC. Therefore, the decomposition temperature of 3TC is decided by the weakest bond within pyrimidine ring.

Molecular bond orders and thermal stability of pyrimidine nucleoside analogs

The calculated weakest molecular bond orders of various pyrimidine nucleoside analogs as well as the accompanying decomposition temperatures (onset) and DTG peak temperatures are listed in Table 1 and presented graphically in Fig. 10. Although the quantum chemical calculation is approximate, there is good correlation between the obtained weakest bond orders of pyrimidine analogs and their corresponding thermal decomposition temperatures,

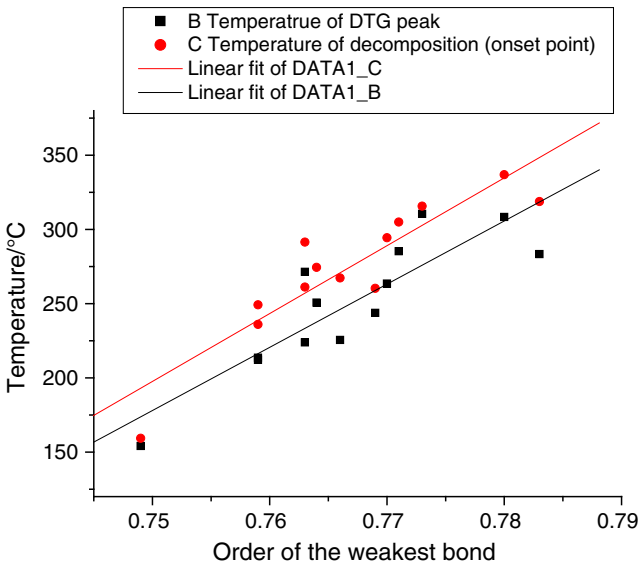

Fig. 10 The relationship between order of the weakest bond and decomposition temperature (onset point) as well as DTG peak

i.e., the bigger the weakest molecular bond order, the higher the initial decomposition temperature and molecular thermal stability.

Conclusions

Our results show that there are four mechanisms for the thermal decomposition of ten pyrimidine analogs studied here. When the peptide bond order is observably lower than that of the weakest bond within pyrimidine ring, the decomposition mechanism is according to mechanism 1, the peptide bond rupture first, and the residue of the thermal decomposition is mainly corresponding pyrimidine. When the peptide bond order is close to that of the weakest bond within pyrimidine ring, the decomposition mechanism is according to mechanism 2, the rupture of the peptide bond and the decomposition of pyrimidine ring synchronize, and the residue of the thermal decomposition contains small amount of corresponding pyrimidine and large amount of insoluble substance. When the peptide bond order is close to that of the weakest bond within pyrimidine ring, and there is oxidation reaction. The decomposition mechanism is according to mechanism 3, such as cytidine. The rupture of the peptide bond, the decomposition of pyrimidine ring, and oxidation reaction synchronize. The residues of the thermal decomposition contain small amount of uridine, cytosine, urical, and large amount of insoluble substance. When the peptide bond order is observably larger than that of the weakest bond in pyrimidine ring, and there is oxidation reaction. The decomposition mechanism is according to mechanism 4, such as 3TC. Most of 3TC decompose first, simultaneously accompanied by the rupture of the peptide bond and oxidation reaction. The residues of the thermal decomposition contain small amount of DTU, cytosine, urical, and large amount of insoluble substance.

Because the peptide bond orders are close to the weakest bonds within the pyrimidine and furan rings, the thermal decomposition of some pyrimidine nucleoside analogs is approximately continuous and synchronous (or partially synchronous). There are large differences between the actual mass loss and the theoretical mass loss at the first stage. The substituent group affects the thermal stability and the thermal decomposition mechanism of the pyrimidine nucleoside analogs. If the electron-donating group is increased on the pyrimidine and furan ring, the peptide bond will be strengthened and the decomposition temperature will rise. There is positive correlation between the molecular orbital bond order calculated by quantum chemistry and the thermal decomposition temperature of the pyrimidine nucleoside analog. The bigger the weakest bond order, the higher the decomposition temperature. Thus, the molecular bond order can serve as the basis to judge molecular thermal stability for analog compounds with similar molecular structure, size, and energy.

Acknowledgements This study was financially supported by Zhejiang Provincial Government of China (No. 2011C11032), and Zhejiang International Studies University (No. 07029005).

References

1. Clercq ED. A 40-year journey in search of selective antiviral chemotherapy. Annu Rev Pharmacol Toxicol. 2011;51:1–24.
2. Galmarini CM, Jordheim L, Dumontet C. Pyrimidine nucleoside analogs in cancer treatment. Expert Rev Anticancer Ther. 2003;3:717–28.
3. Wikipedia. The free encyclopedia. Zidovudine. http://www.en.wikipedia.org/wiki/Zidovudine.
4. Wright K. AIDS therapy. first tentative signs of therapeutic promise. Nature. 1986;323:283.
5. Brook I. Approval of zidovudine (AZT) for acquired immunodeficiency syndrome. J Am Med Assoc. 1987;258:1517.
6. Liu Y, Lin J, Zheng YG, Zhu BQ. Application of zidovudine in cancer therapy. World Clin Drugs. 2012;33:311–3.
7. Wikipedia. The free encyclopedia. Stavudine. http://www.en.wikipedia.org/wiki/Stavudine.
8. Clercq ED. Perspectives for the chemotherapy of AIDS. Chemioterapia. 1988;7:357–64.
9. Lea AP, Faulds D. Stavudine: a review of its pharmacodynamic and pharmacokinetic properties and clinical potential in HIV infection. Drugs. 1996;51:846–64.
10. Wikipedia. The free encyclopedia. Lamivudine. http://www.en.wikipedia.org/wiki/Lamivudine.
11. Bernard B, deceased, Nghe N-B. Use of 1,3-oxathiolane nucleoside analogues in the treatment of hepatitis B. U.S.P. 5532246; 1996.
12. Perry CM, Faulds D. Lamivudine: a review of its antiviral activity, pharmacokinetic properties and therapeutic efficacy in the management of HIV infection. Drugs. 1997;53:657–80.
13. Wikipedia. The free encyclopedia. Telbivudine. http://www.en.wikipedia.org/wiki/Telbivudine.
14. Lai CL, Leung N, Teo EK, Tong M, Wong F, Hann HW, Han S, Poynard T, Myers M, Chao G, Lloyd D, Brown NA. A 1-year trial of telbivudine, lamivudine, and the combination in patients with hepatitis B e antigen-positive chronic hepatitis B. Gastroenterology. 2005;129:528–38.
15. Wang XJ, You JZ. Mechanism and kinetics of thermal decomposition of lamivudine. J Shenyang Pharm Univ. 2010;27:610–4.
16. Wang XJ, You JZ. Thermal decomposition mechanism and kinetics of stavudine. Chin J Appl Chem. 2011;28:709–15.
17. Wang XJ, You JZ. Mechanism and kinetics of thermal decomposition of telbivudine. J Anal Appl Pyrol. 2014;108:228–33.
18. Wang XJ, You JZ. Mechanism and kinetics of thermal decomposition of brivudine. Chin Pharm J. 2014;49(10):899–904.
19. Wang XJ, You JZ. Mechanism of thermal decomposition of zidovudine studied by TGA-FTIR. J Zhejiang Int Stud Univ. 2013;122:1–6.
20. Schmidt MW, Baldridge KK, Boatz JA, Elbert ST, Gordon MS, Jensen JH, Koseki S, Matsunaga N, Nguyen KA, Su S, Windus TL, Dupuis M, Montgomery JA. General atomic and molecular electronic structure system. J Comput Chem. 1993;14:1347–63.
21. Zhuravlev Y, Kravchenko NG, Obolonskaya OS. The electronic structure of alkali metal oxides. Russ J Phys Chem B. 2010;4(1):20–8.

22. Alexeev Y, Mazanetz MP, Ichihara O, Fedorov DG. GAMESS as a free quantum-mechanical platform for drug research. Curr Top Med Chem. 2012;12(18):2013–33.
23. Matos MAR, Sousa CCS, Morais VMF. Thermochemistry of chromone- and coumarin-3-carboxylic acid. J Therm Anal Calorim. 2010;100:519–26.
24. Zayed MA, Hawash MF, Fahmey MA, El-Gizouli AMM. Investigation of ibuprofen drug using mass spectrometry, thermal analyses, and semi-empirical molecular orbital calculation. J Therm Anal Calorim. 2012;108:315–22.
25. Keshavarz MH, Zohari N, Seyedsadjadi SA. Validation of improved simple method for prediction of activation energy of the thermal decomposition of energetic compounds. J Therm Anal Calorim. 2013;114:497–510.
26. El-Gamel NEA, Hawash MF, Fahmey MA. Structure characterization and spectroscopic investigation of ciprofloxacin drug. J Therm Anal Calorim. 2012;108:253–62.
27. Radchenko ED, Sheina GG, Smorygo NA, Blagoi YP. Experimental and theoretical studies of molecular structure features of cytosine. J Mol Struct. 1984;116:387–96.
28. Alemán C. The keto–amino/enol tautomerism of cytosine in aqueous solution. A theoretical study using combined discrete/self-consistent reaction field models. Chem Phys. 2000;253:13–9.